

Small-Scale Planar Nitrous Oxide Monopropellant Thruster for “Green” Propulsion and Power Generation.

Yaniv Scherson¹ and Kevin Lohner¹
Stanford University, Stanford, CA, 94305, USA

Brian Cantwell² and Thomas Kenny³
Stanford University, Stanford, CA, 94305, USA

Research is ongoing at Stanford University on the catalytic decomposition of nitrous oxide as an environmentally friendly monopropellant for propulsion and power applications. Two meso-scale planar monopropellant thrusters have been successfully tested: one made of monolithic silicon carbide utilizing a commercially supplied catalyst, and the other made of Hastelloy-X[®] utilizing a rhodium based catalyst prepared in-house. The unique planar geometry shows a pathway towards scaling down to micro-scale through MEMS-batch fabrication techniques which enable low-cost, mass produced devices with improved thrust to weight ratios and faster start-up transients. The in-house catalyst showed higher reactivity as compared to the commercially supplied catalyst by initiating the decomposition reaction at a temperature of 200°C corresponding to 50W input power. Bed loadings up to 8.67 kg/m²/sec were achieved at a c_{star} efficiency of 71%. Both devices are compared to a previously reported, scaled-up, cylindrical thruster.

Nomenclature

A_o = flow control orifice throat area
 c^* = characteristic exhaust velocity
 C_d = discharge coefficient
 γ = heat capacity ratio
 \dot{m} = mass flow rate
 P_1 = upstream pressure

P_{crit} = static pressure at orifice throat
 P_c = test article chamber pressure
 R_c = universal gas constant
 T_c = test article chamber temperature
 Y = expansion factor
 ρ = density of the gas

I. Introduction

Due to its simplicity, low-cost, and safety, nitrous oxide monopropellant thrusters are ideal for small-scale propulsion applications. Providing a pathway towards micro-scale batch fabrication of planar thrusters enables development of a truly low-cost device with significantly greater thrust to weight ratios and fast start-up transients. A thruster with planar geometry enables a stackable configuration of multiple thrusters to achieve a particular thrust requirement. In a stackable configuration, adjacent thrusters heat one another thus improving decomposition efficiency of the system. This unique configuration allows mass production of low cost thrusters capable of achieving variable thrust requirements. Applications for such a device include: a restartable igniter for larger rocket engines, an oxidizer for an auto-ignitable bipropellant liquid or hybrid rocket engine, a storable monopropellant thruster for satellites, a portable power generating device, and a compact pressurization source for a propellant tank.

Nitrous oxide decomposes exothermically with an adiabatic decomposition temperature of 1640°C and maximum theoretical c_{star} of 1105 m/s. Thermal decomposition of nitrous oxide requires an activation energy of approximately 250 kJ/mol which corresponds to a gas temperature of approximately 850°C, however, this activation energy can be greatly reduced in the presence of a noble metal catalyst. The global decomposition reaction for nitrous oxide is shown below.^{1,2,3,4}

¹Graduate Student, Department of Mechanical Engineering, Stanford, CA, AIAA Member.

²Professor, Department of Aeronautics and Astronautics, Stanford, CA, AIAA Fellow.

³Professor, Department of Mechanical Engineering, Stanford, CA.



It is well known that the presence of a transition metal catalyst can enhance the reaction kinetics of nitrous oxide decomposition and lower the activation energy for decomposition. During the decomposition of N_2O , it is believed that the N_2O molecule adsorbs on a catalyst surface and deposits an oxygen radical on the catalyst surface while N_2 desorbs. The adsorbed oxygen radical can desorb by one of two mechanisms, Eley-Rideal (ER) or Langmuir Hinshelwood (LH). In the ER mechanism, an N_2O molecule collides with an adsorbed oxygen radical and simultaneously desorbs the oxygen radical while decomposing into nitrogen and oxygen gas products. In the LH mechanism, two adsorbed oxygen radicals recombine to form oxygen gas. It is widely accepted that the LH is the predominant mechanisms for catalytic decomposition over transition metal oxides. The LH mechanism suggests that the effectiveness of a catalyst is correlated to the strength of the metal oxygen bond. A catalyst with a strong metal oxygen bond would effectively strip oxygen from the N_2O molecule but limit the rate of oxygen desorption while a weak metal oxygen bond would poorly strip oxygen from the N_2O molecule but easily release adsorbed oxygen. Therefore, the most reactive catalyst has an optimal balance between the strength at which it strips oxygen from N_2O and ease with which it releases adsorbed oxygen. In the case of N_2O decomposition, the period 9 elements in the periodic table have the optimal metal-oxygen bond. It has been found that rhodium and iridium are most reactive in N_2O decomposition. In addition to the surface reactivity, the catalytic decomposition rate is directly proportional to the surface area of the active catalyst. Therefore, a catalyst support with high surface area is important in increasing reaction kinetics.^{4,5,6}

Silicon carbide (SiC) is an extremely high temperature and oxidation resistant material. Deep reactive ion etching (DRIE) of silicon carbide enables this material to be cheaply fabricated in large quantities at micro-scale through MEMS batch etching techniques; therefore, SiC presents itself as a promising chamber material for future micro-scale N_2O monopropellant thrusters.^{7,8,9} However, due to the brittle nature of silicon carbide, meso-scale devices become limited by the maximum allowable chamber pressure. Therefore, this work explores two devices identical in size and dimensions but made from two different materials. One device was fabricated from monolithic silicon carbide (SiC) and the other from Hastelloy-X[®], a high temperature and oxidation resistant nickel based refractory alloy.

II. Experimental Set-Up

The two planar devices shown in Figure 1 were fabricated and hot fire tested in the Stanford lab. The test articles consisted of a rectangular chamber 5 cm long by 3 cm wide by 2 mm thick and a rectangular throat 1 mm by 2 mm. The chamber housed spherical catalyst particles measuring 0.5 mm in diameter. The design point was chosen to produce a chamber pressure of 3.4 atm (50 psia) at a bed loading of 15 kg/m²/sec, a maximum N_2O mass flow rate of 1 gram/sec, and maximum thrust level of 1N. The devices consisted of two rectangular halves sandwiched together and sealed by a thin graphite foil gasket in between. A nickel-chromium resistor coil was placed in the inlet plenum to pre-heat the catalyst bed and initiate the decomposition reaction. LEM[®] voltage and current sensors attached to the heating coil leads were used to measure the power supplied. Four Omegaclad[®] XL thermocouple probes supplied by Omega[®] were used. One thermocouple was used to measure upstream sonic orifice temperature in the nitrous oxide feedline. A second thermocouple was placed at the forward end of the catalyst bed embedded inside the pre-heat coil and just below the gas flow inlet as shown in Figure 2 left. This thermocouple was used to detect local reaction initiation. The third thermocouple was placed just upstream of the nozzle at the chamber centerline to measure chamber temperature. The fourth thermocouple was placed midway between the chamber wall and the chamber centerline to measure the temperature gradient between the center and side flows, Figure 2 left. Laser-drilled ruby orifices from Bird Precision[®] were used to meter the flow rate to desired levels. The discharge coefficients of the orifices were determined through calibration by measuring tank mass before and after several cold flow tests. The catalyst was restrained on the aft end by a silicon carbide foam disc. Instrumentation ports and fluidic interconnects were welded onto the main body.

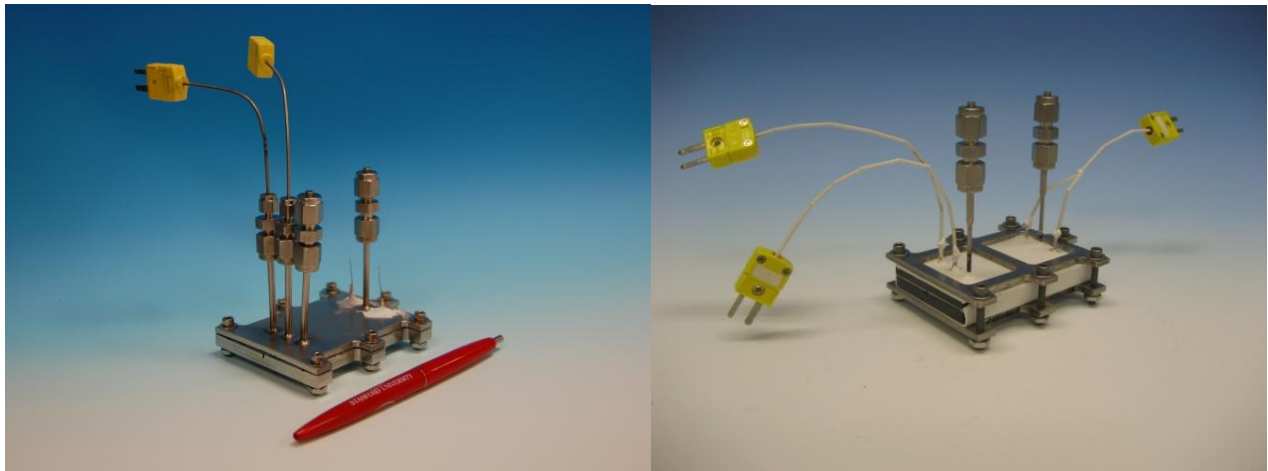


Figure 1: Pictures of two different devices tested. Hastelloy-X device with in-house made catalyst (left) and silicon carbide device with commercially supplied catalyst (right).

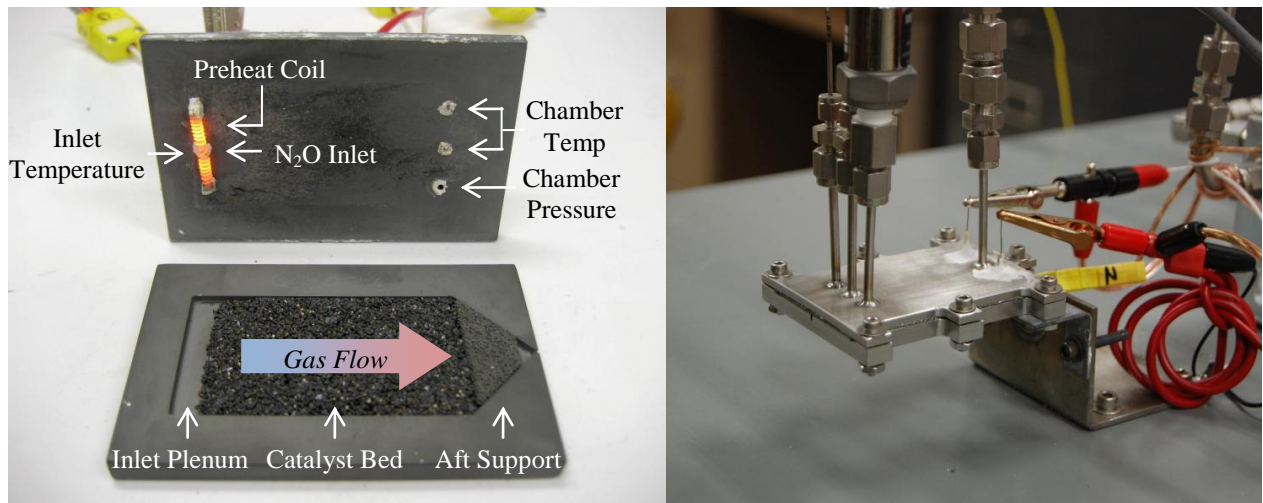


Figure 2: View of chamber of silicon carbide device loaded with catalyst, interior instrumentation ports, and interior components (left). Picture of Hastelloy-X[®] device mounted on test bed (right)

Two different catalysts were tested in each device. The silicon carbide device was loaded with a commercially supplied catalyst while the Hastelloy-X[®] device was loaded with a rhodium based catalyst that was prepared in-house following the methods described in previous works.^{10,11} Gamma-alumina spheres, 0.5 mm in diameter and 170 m²/gram surface area, were coated with the metal oxide catalyst. SEM pictures in Figure 3 reveal the highly porous gamma-alumina catalyst support coated with metal oxide. As can be seen in the pictures, the metal catalyst formed both an oxide coating and granular particles, which result in higher catalyst surface area. It is interesting to note that some of the cavities of the support appear to be covered; it is possible that the effective surface area of the catalyst was decreases thus reducing the effectiveness of the catalyst.

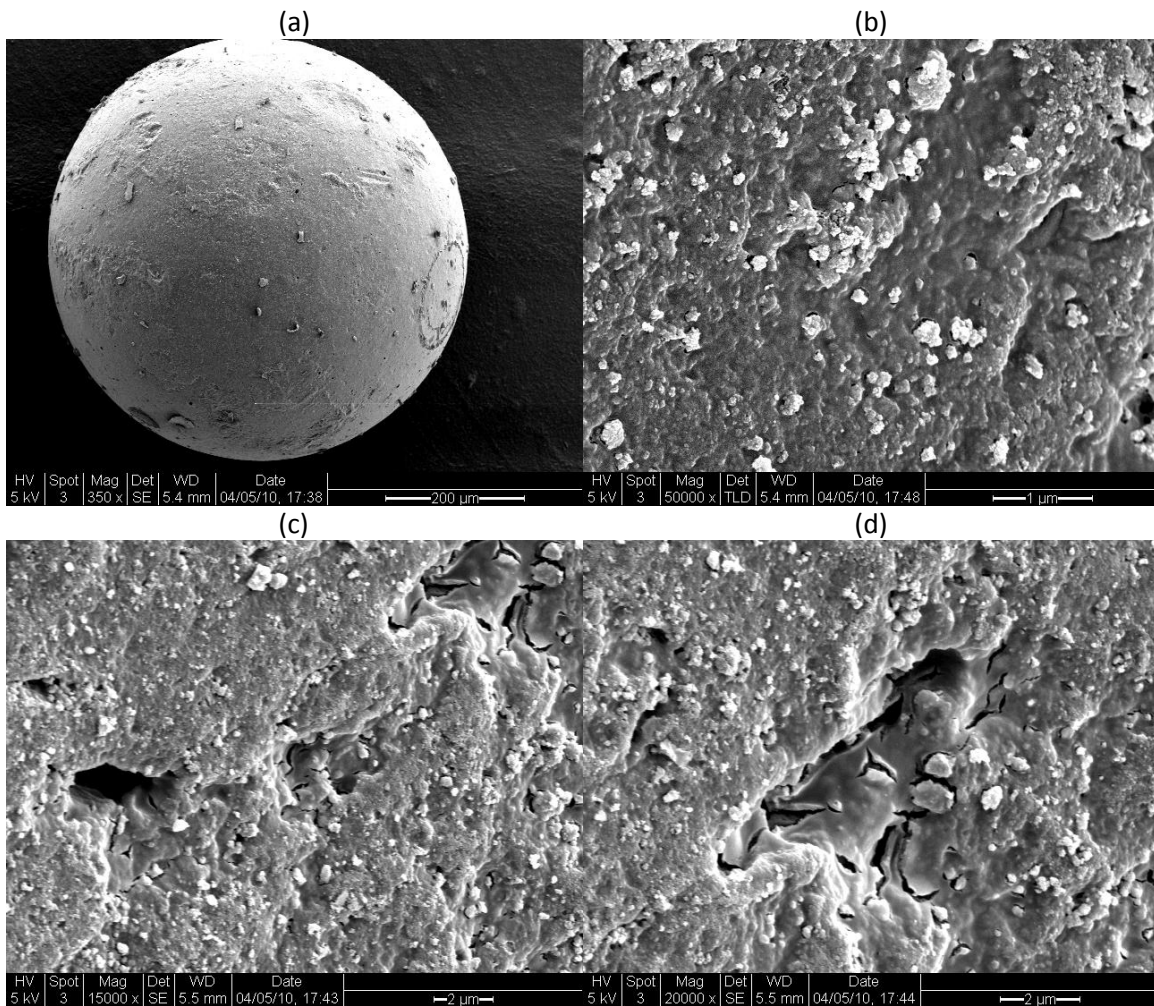


Figure 3: SEM pictures of in-house made catalyst tested in Hastelloy-X[®] device. (a) Wide view of a single alumina spherical support coated with metal oxide catalyst (b) Zoomed-in images revealing formation of granular catalyst particles (c) & (d) Zoomed-in images revealing partial coverage of support surface area.

III. Hot Fire Testing

Multiple hot fire tests were conducted on each device. Both devices achieved steady state catalytic decomposition of nitrous oxide. A nickel-chromium coil inserted in the plenum at the forward end of the catalyst bed was used to preheat the catalyst while nitrous oxide was flowed through the device. Once sufficient activation energy was inputted to initiate the reaction, the preheat coil was shut off. Following reaction initiation, nitrous oxide flow was throttled to various set flow rates and held at steady-state to obtain bed loading and c^* efficiency measurements. Due to the higher surface area to volume ratio of the planar chamber geometry, as compared to cylindrical chamber geometry, the devices were unable to achieve design point bed loading and high c^* efficiencies. However, the decomposition reaction was successfully initiated in both devices at low input power and low chamber temperatures. Steady-state operation was also achieved in both devices as shown in the hot fire test pictures in Figure 4.

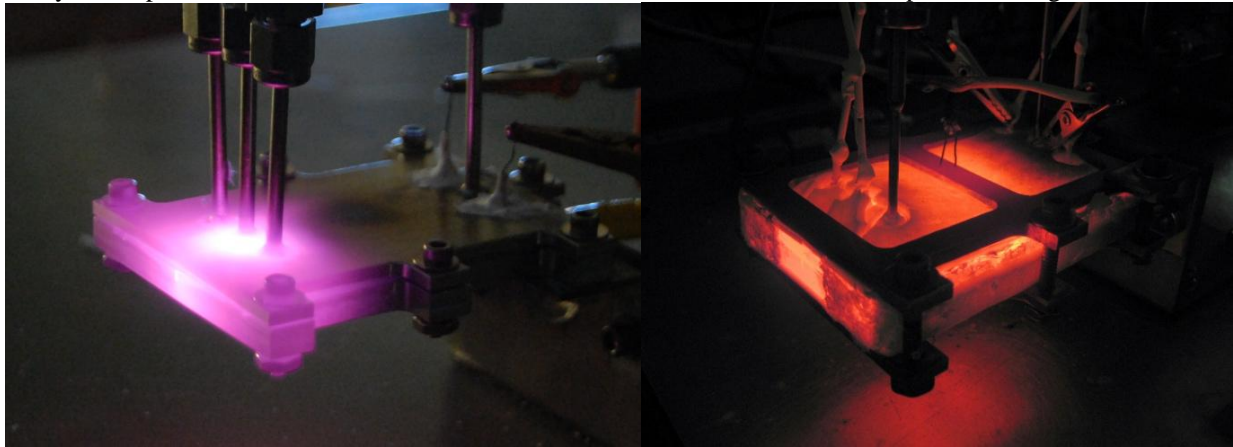


Figure 4: Hot fire test pictures of Hastelloy-X[®] device with in-house made catalyst (left) and silicon carbide device with commercially supplied catalyst (right).¹²

Figure 5 and Figure 6 show temperature and mass flow rate test profiles of the Hastelloy-X[®] device loaded with in-house made catalyst and the silicon carbide device loaded with commercially supplied catalyst. The in-house made catalyst required a preheat temperature of approximately 200°C, corresponding to 50W supply power, in order to initiate the decomposition reaction while the commercially supplied catalyst required a preheat temperature of approximately 400°C, corresponding to 100W supply power. The catalyst prepared in-house demonstrated significantly higher reactivity during device start-up. The catalyst prepared in-house achieved a maximum chamber temperature of 610°C while the commercially supplied catalyst achieved a maximum chamber temperature of 820°C. However, the silicon carbide device which housed the commercially supplied catalyst was insulated with a single layer of 1/8" thick aluminum oxide felt while the Hastelloy-X[®] device which housed the in-house made catalyst was unable to be insulated with the felt due to reaction between the metal device and felt material. This could explain the disparity in maximum achieved chamber temperature. The chamber temperature gradient between centerline and midway between centerline and chamber wall was consistently 10°C, therefore, the decomposition reaction remained nearly homogeneous.

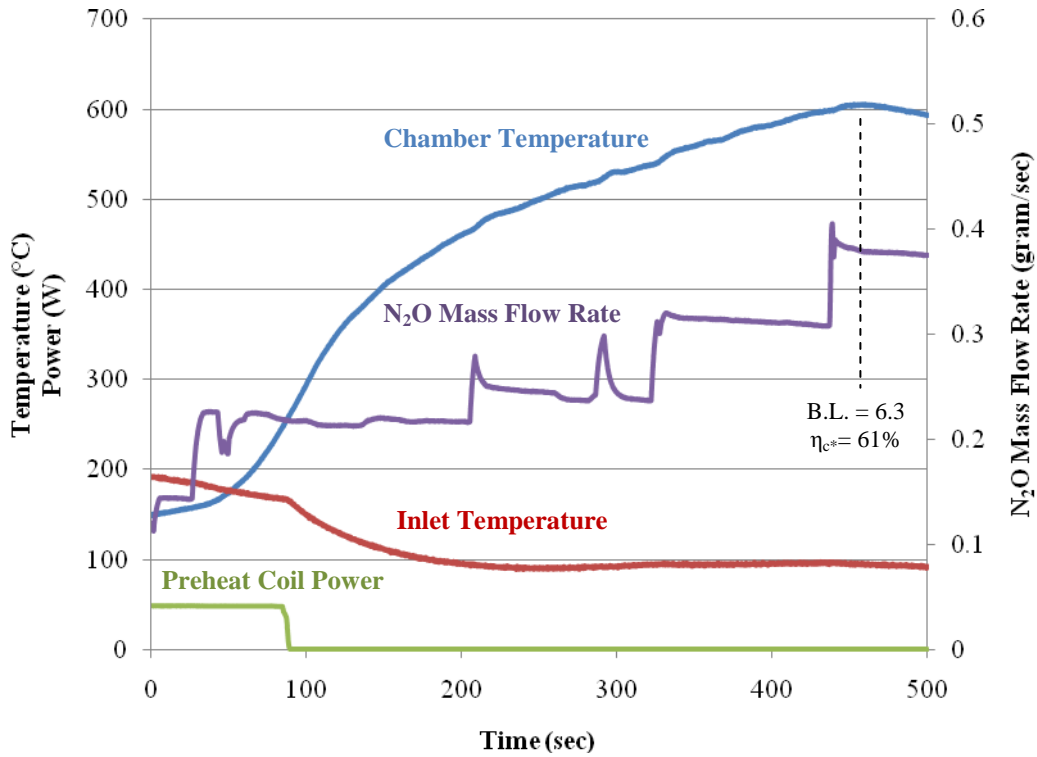


Figure 5: Test profile of Hastelloy-X[®] device loaded with in-house made catalyst. Bed loading, B.L., ($\text{kg}/\text{m}^2/\text{sec}$) and maximum c_{star} efficiency, η_{c^*} , are shown.

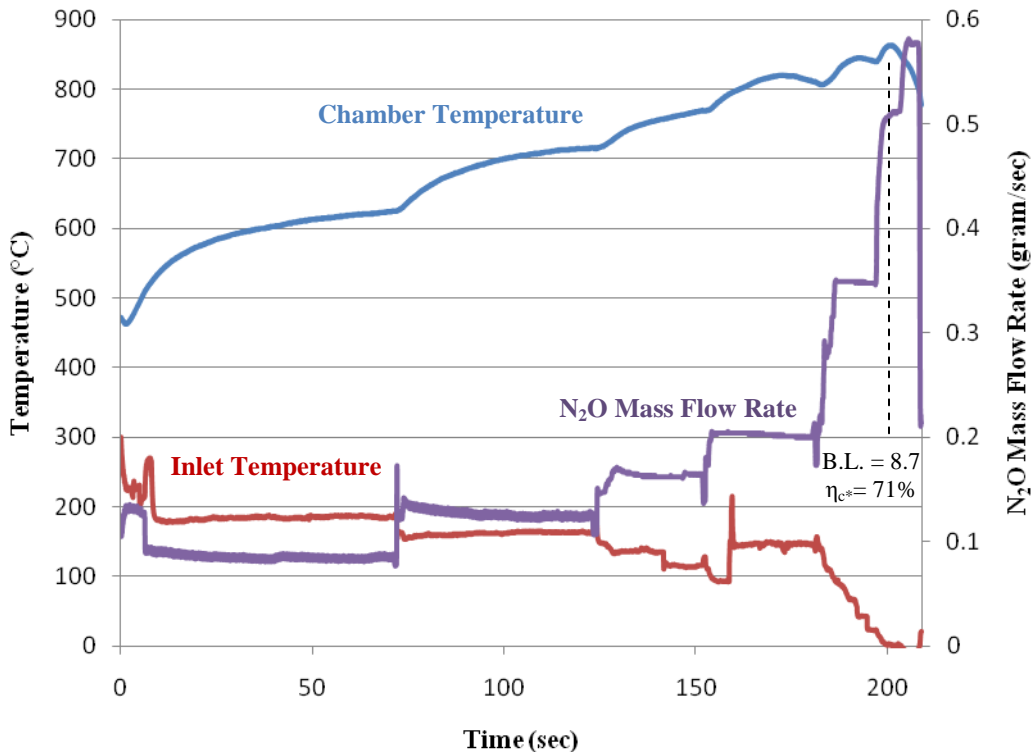


Figure 6: Hot fire test profile of silicon carbide device loaded with commercially supplied catalyst. Bed loading, B.L., ($\text{kg}/\text{m}^2/\text{sec}$) and maximum c_{star} efficiency, η_{c^*} , are shown.

For comparison, the in-house made catalyst was tested in a scaled-up cylindrical device described in previously published work that tested the commercially supplied catalyst.⁶ Figure 7 shows a test profile of this scaled-up device achieving decomposition temperatures over 1000°C and a maximum c_{star} efficiency of 80%, confirming the high reactivity of the in-house made catalyst.

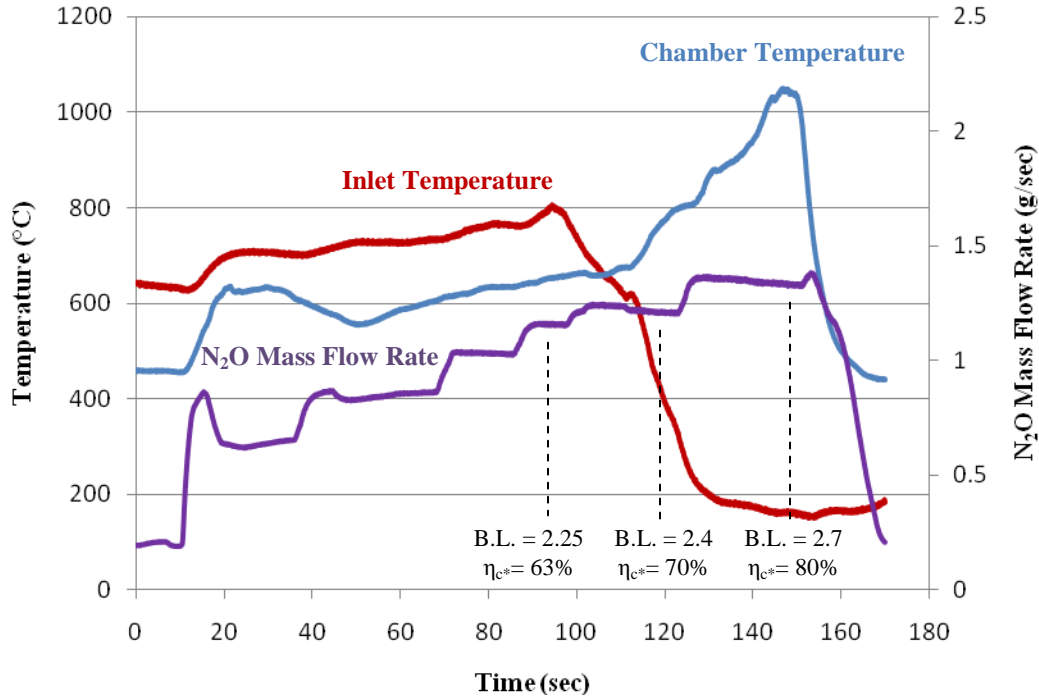


Figure 7: Test profile of scaled-up cylindrical thruster with in-house made catalyst (Device from previously published work). Bed loading, B.L., ($\text{kg}/\text{m}^2/\text{sec}$) and c_{star} efficiencies, η_{c^*} , are shown.⁶

IV. Data Analysis

At each time step, instantaneous nitrous oxide density was calculated from the measured feedline pressure and temperature using the NIST database.¹³ This density was then used to calculate the mass flow rate based on equation 3 below.

$$\dot{m} = Y \cdot C_d \cdot A_o \sqrt{2 \cdot \rho \cdot (P_1 - P_{crit})} \quad (2)$$

At specific steady state points during each test, the characteristic exhaust velocity (c_{star}) and bed loading (B.L.) was calculated from the decomposition temperature and mass flow rate, respectively, as shown below.

$$c_{star} = \frac{\sqrt{\gamma_{N_2O} \frac{R_c}{MW_{prod}} T_c}}{\gamma_{N_2O} \sqrt{\left(\frac{z}{\gamma_{N_2O} + 1}\right) \gamma_{N_2O}^{-1}}} \quad (3)$$

$$B.L. = \frac{\dot{m}_{N_2O}}{A_{ch}} \quad (4)$$

Where γ_{N_2O} is the heat capacity ratio of N_2O , MW_{prod} is the average molecular weight of the decomposition products, \dot{m}_{N_2O} is the mass flow rate of N_2O , and A_{ch} is the cross sectional area of the device chamber. The c_{star} efficiency is the ratio of the experimentally determined c_{star} and ideal c_{star} at the adiabatic decomposition temperature. The maximum performance parameters achieved in each device is summarized below in Table 1.

Table 1: Maximum mass flow rate, bed loading, chamber temperature, c^* , and c^* efficiency achieved in each device.

	Max \dot{m}_{N_2O} (gram/sec)	Max B.L. (kg/m ² /sec)	Max T_{ch} (°C)	Max c^* (m/s)	Max c^* efficiency
Silicon Carbide (commercial catalyst)	0.52	8.67	820	834	71%
Hastelloy-X[®] (in-house catalyst)	0.38	6.33	610	749	61%
Scaled-Up cylindrical Thruster (in-house catalyst)	1.38	2.70	1043	915	80%

V. Conclusions

The successful testing of the silicon carbide and Hastelloy-X[®] devices proves the feasibility of sustaining a decomposition reaction in a chamber of planar geometry and provides a pathway for fabricating future micro-scale devices from monolithic silicon carbide. Micro-scale devices would benefit from increased thrust to weight ratios, faster start-up transients, and low-cost bulk fabrication. Although the high surface area to volume ratio of a single thruster limits the maximum decomposition chamber temperature, improved insulation and the stacking of multiple devices that heat one another would increase chamber temperature and improve decomposition efficiency thus allowing for higher bed loadings and thrust.

As compared to the commercially provided catalyst, the catalyst made in-house demonstrated higher reactivity at lower start-up temperatures and achieved comparable performance parameters. The successful testing of the in-house made catalyst provides a much lower cost alternative to commercial catalysts.

Acknowledgements

Financial support, materials, and equipment for this research were provided by the Woods Institute for the Environment at Stanford University and the Stanford University Department of Aeronautics and Astronautics.

References

- [1] K. Lohner, J. Dyer, E. Doran, Z. Dunn, B. Krieger, and V, "Design and Development of a Sub-Scale Nitrous Oxide Monopropellant Gas Generator," 43rd AIAA/ASME/SAE/ASEE Joint Propulsion Conference & Exhibit, AIAA, Cincinnati: 2007, pp. 1-10.
- [2] V. Zakirov, M. Sweeting, V. Goeman, and T. Lawrence, "Surrey research on nitrous oxide catalytic decomposition for space applications," 14th AIAA/USU Conference on Small Satellites, 2000, pp. 1-9.
- [3] P. Atkins and L.L. Jones, Chemistry: Molecules, Matter, and Change, New York: W. H. Freeman and Company, 1997.
- [4] F. Kapteijn, J. Rodriguezmirasol, and J. Moulijn, "Heterogeneous catalytic decomposition of nitrous oxide," Applied Catalysis B: Environmental, vol. 9, 1996, pp. 25-64.
- [5] Y. Li and J.N. Armor, "Catalytic decomposition of nitrous oxide on metal exchanged zeolites," Applied Catalysis B: Environmental, vol. 1, 1992, pp. L21-L29.
- [6] Y. Scherson, K. Lohner, B. Lariviere, B. Cantwell, and T. Kenny, "A Monopropellant Gas Generator Based on N₂O Decomposition for "Green" Propulsion and Power Applications," 45th AIAA/ASME/SAE/ASEE Joint Propulsion Conference & Exhibit, Denver: AIAA, 2009, pp. 4875-4875.
- [7] G. Beheim and C. Salupo, "Deep RIE Process for Silicon Carbide Power Electronics and MEMS," Materials, vol. 622, 2001, pp. 1-6.
- [8] R. Okojie, R. Tacina, C. Wey, and C. Blaha, "Micro fabrication of SiC mesoscale lean direct injector array: Toward active combustion control," Solid-State Sensors, Actuators and, 2007, pp. 2433-2436.
- [9] I. Behrens, E. Peiner, A. Bakin, and A, "Micromachining of silicon carbide on silicon fabricated by low-pressure chemical vapour deposition," Journal of Micromechanics and Microengineering, vol. 12, 2002, pp. 380-384
- [10] K. Yuzaki, "Catalytic decomposition of N₂O over supported Rh catalysts: effects of supports and Rh dispersion," Catalysis Today, vol. 45, 1998, pp. 129-134.
- [11] T. Nobukawa, M. Yoshida, S. Kameoka, S. Ito, K. Tomishige, and K. Kunimori, "Role of nascent oxygen transients in N₂O decomposition and selective catalytic reduction of N₂O," Catalysis Today, vol. 93-95, 2004, pp. 791-796.
- [12] K.A. Lohner and Y.D. Scherson, "Nitrous Oxide Monopropellant Gas Generator Development," 3rd Spacecraft Propulsion Joint Subcommittee Meeting, JANNAF, 2008.
- [13] R. Reid, J. Prausnitz, and B. Poling, Properties of Gases and Liquids, New York: McGraw-Hill Book Company, 1987.